

# Wind tunnel testing of a wind turbine in complex terrain

Emmanouil M Nanos<sup>1</sup>, Kutay Yilmazlar<sup>1</sup>, Alex Zanotti<sup>2</sup>, Alessandro Croce<sup>2</sup> and Carlo L Bottasso<sup>1</sup>

<sup>1</sup>Wind Energy Institute, Technische Universität München, Garching bei München, Germany.

<sup>2</sup>Dipartimento di Scienze e Tecnologie Aerospaziali, Politecnico di Milano, Milano, Italy.

E-mail: [em.nanos@tum.de](mailto:em.nanos@tum.de)

**Abstract.** The paper describes the development of a scaled model of complex terrain, suitable for terrain-wind turbine interaction wind tunnel studies, taking into account flow similarity criteria. The size and the geometry of the experimental model of the complex terrain were refined using results of CFD simulations in order to achieve the best possible flow similarity and avoid edge effects arising from the finite (relative to the rotor size) terrain geometry. Moreover, Particle Image Velocimetry was used to survey the flow field on a longitudinal plane along the terrain center line. Flow measurements with and without a wind turbine model enabled to quantitatively evaluate the speed up produced by the terrain in the region of the wind turbine and the effect of the terrain on the wake characteristics of the wind turbine model.

## 1. Introduction

As the share of on-shore wind energy grows rapidly in the global energy mix, turbines are installed on complex sites more and more frequently [1]. It is well known that complex terrain may have considerable effects on the flow within a wind farm, affecting the conditions that a turbine is experiencing. Therefore, accurate micro-siting plays a crucial role for wind farm design and estimation of power production in such landscapes. Studies have shown that even relatively minor errors during the planning phase could lead to considerable losses in annual energy production [2]. Yet, the mathematical models that are commonly used for wind energy systems are not fully validated for complex topographies [3]. Even in the two-dimensional case, it has been shown that linear theories describing the flow over hilly terrains are not sufficiently precise [4]. In a complex terrain with 3D elevation gradients, an erroneous flow prediction might have even higher impact on wind turbine micro-siting. As a consequence, it is necessary to increase the level of understanding of flows over complex terrains so that better flow models can be developed for landscapes where three-dimensional variability of wind characteristics is anticipated [5].

There is a number of studies on flows over complex topographies, typically hills and escarpments, dealing with the topic both from the numerical and experimental points of view [6, 7, 8], while there are some purely numerical studies on wind turbine complex terrain interaction [9, 3, 10, 11]. However, there is a lack of experimental studies that combine complex terrain and wind turbines and can provide benchmark measurements. The studies by Hyvärinen et al. [12] and Tian et al. [13], who used idealized two-dimensional terrain models, are the sole



examples, yet they used simplified geometries with low Reynolds flows. Combining relatively high Reynolds complex terrain and a fully controllable wind turbine requires careful design of the set-up, with the literature lacking relevant examples. This paper aims at filling this gap by presenting the design of a wind tunnel study of a complex terrain coupled with a wind turbine. To this purpose, a scaled model of a real test site is designed and manufactured with the goal of producing an experimental set-up that provides an as-realistic-as-possible flow while satisfying the constraints given by the wind tunnel and the measuring equipment. Following this, PIV measurements are performed as a preliminary analysis of the flow behaviour over the terrain with and without the presence of a scaled wind turbine model. The goal is to validate an experimental set-up that can contribute to a better understanding of turbine-terrain interaction in terms of wake behavior and turbine performance, and to provide data for the validation of numerical codes. The paper is organized as follows: in section 2 the methodology followed for the design of the terrain is described, section 3 presents the wind tunnel measurement results, while section 4 provides the most significant conclusions of this work along with the next steps on this project.

## 2. Terrain design methodology

### 2.1. Design of terrain model

The terrain model is based on a test site located in Stöttener Berg close to Gieslingen in Baden-Württemberg, in the south-west of Germany. Over the past years, this site has been home to wind energy research projects such as KonTest and WINSSENT. Within the scope of these projects, site measurements have been executed involving met masts, Lidars and unmanned aerial vehicles at various locations [14, 15]. Two research wind turbines are planned to be installed close to the escarpment for further wind turbine-terrain interaction studies. The terrain consists of a densely forested steep escarpment, showing a relative elevation of ca. 200 m and slopes up to  $30^\circ$ , and a relatively flat plateau with minor vegetation following the slope. The main wind direction is reported at  $295^\circ$  [14]. A digital elevation of the terrain, aligned with the main wind direction, is shown in Fig. 1. A red frame outlines the portion represented by the wind tunnel model, while a red x symbol reports the turbine position (WT), where the dimensions are given in rotor diameters. In the initial stage of the terrain design, the width of the terrain was chosen to be 7 rotor diameters as a compromise between low blockage (which requires a small width) and effect on the flow (which requires a larger width). In order to ease the manufacturing of the terrain model and the execution of the experiments, the terrain is divided into two parts as labelled in the terrain elevation profile in Fig. 2. The plateau starting from the red dashed line is considered to be completely flat in the present study.

Given the confined space of the wind tunnel, the terrain will have, contrary to the real test field, finite dimensions relative to the size of the turbine. It is therefore necessary to optimize the shape and size of the terrain in a way that edge effects are minimized while blockage is kept as low as possible. To analyse the effects of model boundaries on the flow behaviour, a set of model geometries, which is given in Fig. 3, was simulated via Large Eddy Simulations performed

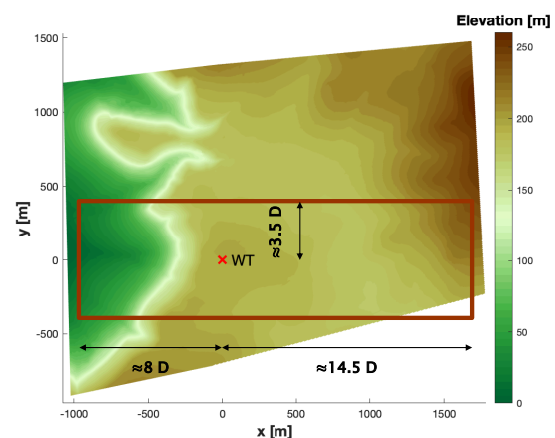


Figure 1: Modelled area on topographic map.

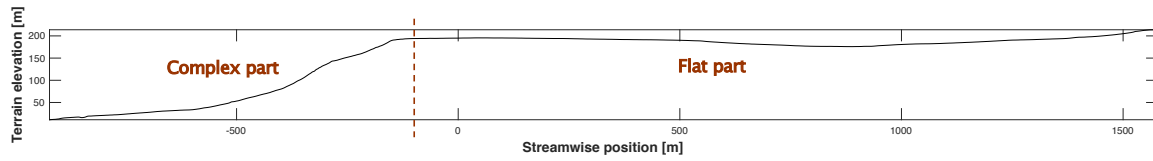


Figure 2: Elevation profile along a plane passing through the center of the wind turbine rotor. The red dashed line indicates the transition point from complex part to flat part.

in *OpenFOAM*. The model geometries are simplified 2D versions of the actual complex model, and were generated by extruding the elevation profile at the edge of the complex part along the lateral direction. This way, the effect of the side boundaries on the flow is isolated from 3D spatial variations of the terrain for a better analysis. Each model holds the same overall dimensions: 6 x 1 x 13.5 m, along width, height and length, respectively. The implemented numerical setup is based on an in-house developed LES framework, which has been validated against wind tunnel measurements [16], [17].

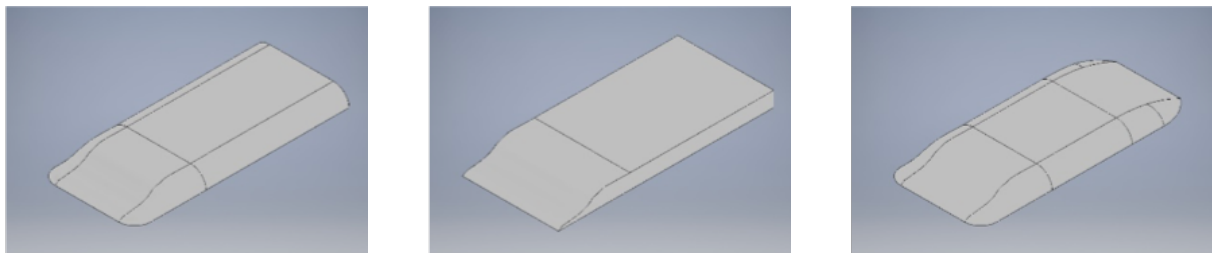


Figure 3: Terrain geometries in comparison: Model A (*left*), Model B (*middle*) and Model C (*right*).

Figure 4 presents a comparison of vorticity magnitudes between Model A and B on the cross-flow plane at the turbine position. As expected, sharp corners induce large vortices at the lateral edges of the model. These vortices are in reality not present in the test field. Since the presence of vortices might influence the flow around the measurement plane and their area of influence is likely to get bigger as they travel downstream, Model A was chosen over Model B.

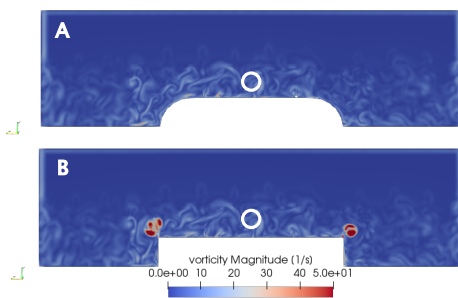


Figure 4: Vorticity comparison: cross-flow plane at rotor position. The white circle indicates the rotor disk.

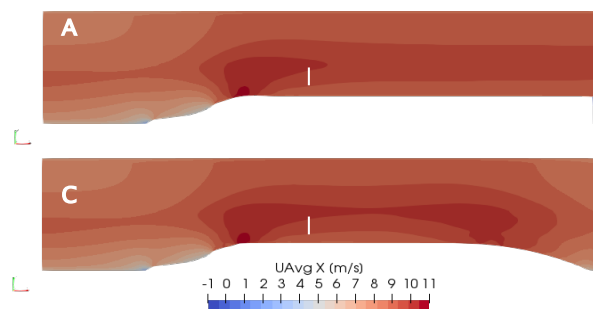


Figure 5: Average velocity comparison: longitudinal plane at rotor center position. The white line indicates the rotor disk.

Another comparative analysis was performed between Model A and C with respect to the back shape of the model. The average velocity fields on the longitudinal plane at the turbine position are presented in Fig. 5. The turbine rotor is indicated with a white line. As shown in the figure, Model C causes a flow acceleration at the beginning of the curved shape at the back of the model. A similar acceleration is reported far downstream of the Bolund Hill plateau before reaching the lee side of the hill in a wind tunnel experiment [18]. Besides, Model A exhibits a more homogeneous flow field behind the turbine, and possible perturbations to the flow caused by the edges of the model and measurement equipment are pushed to the end of the test section by keeping the terrain flat for another 2.5 meters.

### 2.2. Flow similarity

Given that the purpose of the study is to model atmospheric flow in a wind tunnel, it is necessary to assess how the wind tunnel flow is similar to a full scale flow. This was attempted here through a set of dimensionless numbers derived from the Navier-Stokes equations, namely the Reynolds, Richardson, Eckert, Rosby and Prandtl numbers. For the derivation and physical importance of each number the reader can refer to Cermac and Durst [19, 20]. Regarding the Reynolds number, the geometric scaling factor of the terrain is 1:195, which is a relatively large one compared to previous complex-terrain-only studies. In fact, it is well above the minimum scale factor 1:500 for wind modelling over complex terrains recommended by Bowen [21]. Considering an inflow speed of around 8 m/s at hill height, the Reynolds number with respect to hill height  $Re_H$  equals ca.  $5.14 \times 10^5$ , which is the highest  $Re_H$  reported in the literature and, according to the findings of McAuliffe and Larose [22], is beyond the threshold for *Re-independent* flow. What is more, with this geometric scaling factor the wind turbine model, which has a  $D = 0.6$  m rotor diameter, resembles a typical full-scale on-shore wind turbine.

Since the wind tunnel can produce a neutrally stratified boundary layer, Richardson and Eckert similarity is satisfied. Furthermore, given the fact that the longitudinal length scale of the terrain model (2.6 km at full-scale) is below the maximum limit of 5 km for negligible Coriolis effects [23], Rossby number similarity can be neglected. Finally, the medium of the flow is air, so that Prandtl similarity is also satisfied.

### 2.3. Evaluation of blockage effects

The selected terrain geometry with curved side shapes and a backward facing step has a blockage ratio of 10% in the Atmospheric Boundary Layer (ABL) wind tunnel of Politecnico di Milano, which has a cross section of 13.84 m x 3.84 m. In general, blockage effects can be neglected when the blockage ratio is lower than 5% [24]. Since the present terrain model exceeds this safe limit, the blockage effects should be quantified. At this aim, two CFD analyses have been considered: the first models the correct wind tunnel geometry as implemented for Model A in the previous section, while a second one, with a *blockage-free* configuration, is implemented by extending the wind tunnel domain up to a cross-section of 25 m x 9 m (ca. 1.8 times the actual width and 2.3 times the actual height of the wind tunnel). Hereby, blockage ratio is reduced to 2.5%, which means that blockage effects are negligible. Blockage analysis was performed with steady RANS simulations in *Ansys Fluent* using the standard  $k-\epsilon$  turbulence model.

The streamwise velocity component  $U_x$  is plotted on longitudinal and lateral planes in Fig. 6. It is clear that the wind tunnel blockage has some influence on the results. A point to point comparison of the results from both models reveals that the turbine rotor is experiencing a 5% higher wind speed in the wind tunnel than it would in an open free-stream environment, a fact that should be taken into account when analysing the experimental data.

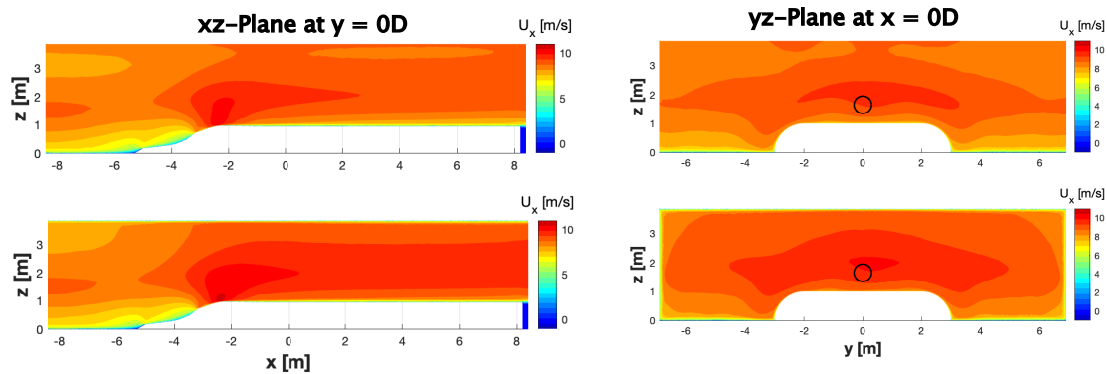


Figure 6: Blockage effects on average velocity field. Top row: results from blockage-free configuration; bottom row: results from model with actual wind tunnel geometry.

#### 2.4. Manufacturing of the terrain

The complex terrain model was divided into 9 sub-parts with dimensions around 1.35 m x 1.5 m (width x length), to conform to the CNC machine operational range and for transportability. Polystyrene foam (EPS) with a density of 20 kg/m<sup>3</sup> was selected as material based on low cost, low weight and millability. Each part was cut from a block of EPS by a 5-axis-CNC machine starting with a 40 mm diameter spherical cutter to give an initial coarse shape (see Fig. 7), and then refining the surface with an 8 mm diameter spherical cutter.



Figure 7: A complex sub-part cut by CNC machine.

Thanks to the small tolerance range of the CNC machine ( $\pm 0.15$  mm) and the high resolution digital elevation model (grid spacing equal to 5mm), a very precise terrain model was produced. Since  $Re_H$  is high enough to ensure a turbulent boundary layer and, consequently, avoid laminar separation issues, the model surface was kept smooth without any additional roughness elements or terraced shapes, which have been used to enhance transition to turbulent boundary layer in previous complex terrain studies [22, 6]. Due to limitations of the minimum thickness that can be produced at the lowest point of the model, an upward offset of 20 mm had to be realized. Furthermore, the upstream parts were glued on a 4 mm thick plywood to prevent the flow to leak

under the model. In total, the height of the model is increased by 24 mm to approximately 97 cm.

For the rest of the model, a lighter and cheaper EPS with a density of 10 kg/m<sup>3</sup> was used. To reduce the costs, these parts were cut by a hot-wire-cutter with a lower precision. For the curved side shapes, 8 cross sections along the length of the complex part were used. Rectangular blocks of foam were used to realise the flat part of the model. Their top surfaces were covered with thin plywood sheets, for ensuring structural integrity and for allowing safe access to the flat surface during experiments. In the middle line of the test section, a thick wooden platform, mounted on an aluminium frame, was constructed to support the model and all the measuring equipment. After mounting all the model components in the wind tunnel, their adjacent edges were taped together in order to block possible flow paths through the terrain model. The final

layout of the experiment can be viewed in Fig. 8.

### 3. Wind tunnel measurements

#### 3.1. Experimental set-up

The experiments were conducted in the ABL test section of the wind tunnel at Politecnico di Milano. The flow field was measured with a PIV system arranged on a vertical plane at the hub height and parallel to the flow, on a rectangular plane of size approximately  $4 D \times 2 D$  (see Fig. 9). The PIV equipment included a Nd:Yag double pulsed laser with 200 mJ/pulse and a 2 Mpx double shutter camera mounted on a traversing system to span the entire measurement area. The total investigated domain of about  $3 \text{ m} \times 1.2 \text{ m}$  is one of the largest areas that have been examined via PIV so far [2]. The total measurement area was composed by twelve windows with

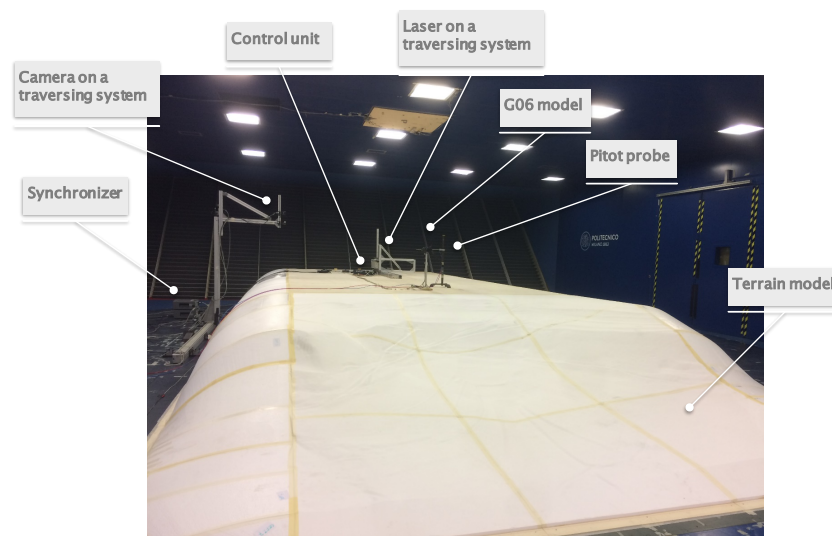


Figure 8: Experimental set-up.

a size of approximately  $0.75 \text{ m} \times 0.4 \text{ m}$ . For each measurement window, 1000 image pairs were captured. Throughout the measurement campaign, two set of measurements were performed. First, the flow over the terrain was investigated without the turbine. Next, a G06 turbine was installed close to the escarpment ( $1 D$  downwind from the edge of the slope), similarly to the position of one of the WINSSENT turbines at full-scale. The scaled wind turbine (G06) used in this work is a three bladed model with a  $0.6 \text{ m}$  rotor designed for studies on wakes and wind farm control. It is equipped with manually pitched low Reynolds (RG-14 airfoil) carbon fibre blades, strain gauges at tower base to measure the tower bending loads and a torque-meter to measure the torque on the main shaft. More details about the design, performance and wake characterization of the model can be found in [25] and [26]. The wind turbine was operated at its optimum tip speed ratio and pitch angle throughout all experiments reported here.

A turbulent inflow was generated with the use of spires at the inlet of the wind tunnel test section and bricks used as roughness elements placed on the tunnel floor upwind of the terrain model for a length of approximately  $20 \text{ m}$ , about 20 times the hill height. With the given turbulent inlet configuration, the resulting inflow velocity profile is presented in Fig. 10, where the vertical coordinate is normalized by the hill height  $H$ . Measured velocity values (red stars) were obtained from a Pitot tube  $2.5 \text{ m}$  upstream of the terrain model, where the ABL is fully developed and the flow is not yet influenced by the terrain. The incoming velocity at hub height ( $z_{HH} = 1.58 \text{ m}$  above wind tunnel floor) is  $8.7 \text{ m/s}$ , while the turbulence intensity is  $8.77 \%$  at hub height and  $11.54 \%$  at the hill height level. Measured values are fitted with

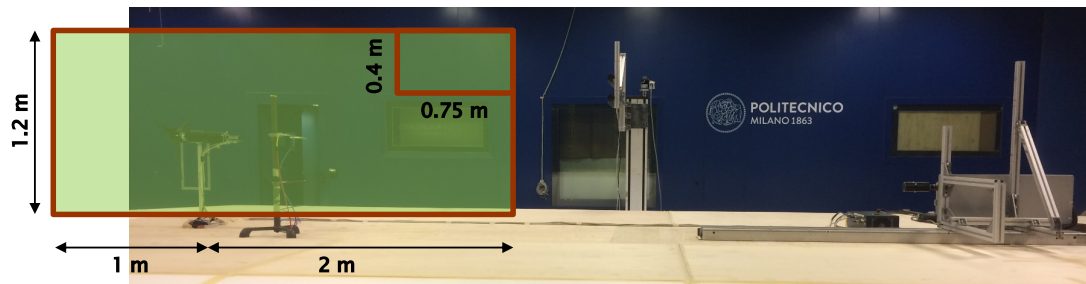


Figure 9: Measurement plane (side view of terrain model).

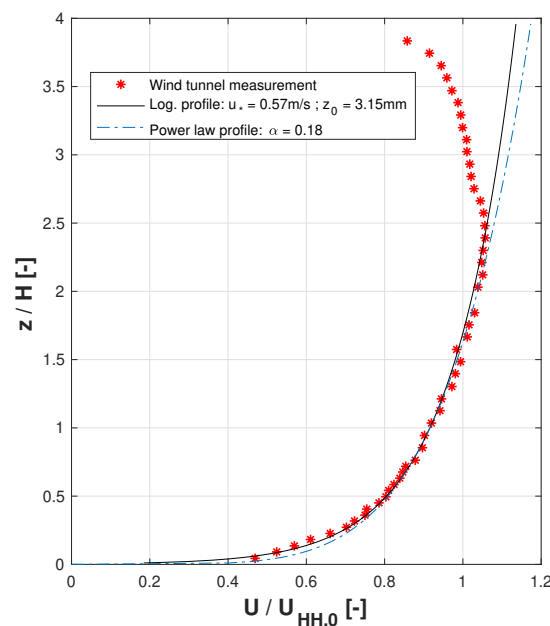


Figure 10: Inflow velocity profile.

a logarithmic wind profile with friction a velocity  $u_* = 0.57$  m/s and a surface roughness  $z_0 = 3.15$  mm. The best match is obtained by power law exponent  $\alpha = 0.18$ , which is in line with a roughness length classification *moderately rough*, according to VDI guidelines [24]. The ABL profile with this  $\alpha$  value builds up above *grassland* terrain, which is, in fact, present in the upwind region of the escarpment. At the light of the wind profile parameters, a high surface Reynolds number  $Re_* = u_* \times z_0 / \nu = 119$ , similar to the one reported by Conan et al. [6], ensures an aerodynamically rough (in other words, fully turbulent) flow.

### 3.2. Results

Velocity data obtained by PIV for the case without the turbine is visualized in Fig. 11. The origin of the reference system used to report the PIV results is at the rotor hub center. The contour plots of the free-stream velocity component show that the flow reaches its highest speed at the edge of the escarpment, due to the blockage caused by the terrain. At this point, the flow has a low shear, hence a relatively uniform velocity profile. Afterwards, it loses speed along the plateau, where a boundary layer starts developing. The vertical velocity field in Fig. 11 at right reveals that the flow has a vertical component equal to about 20% of the inflow speed, due

to the steep slope of the terrain. However, this vertical component is considerably diminished before reaching the turbine position ( $x/D = 0$ ).

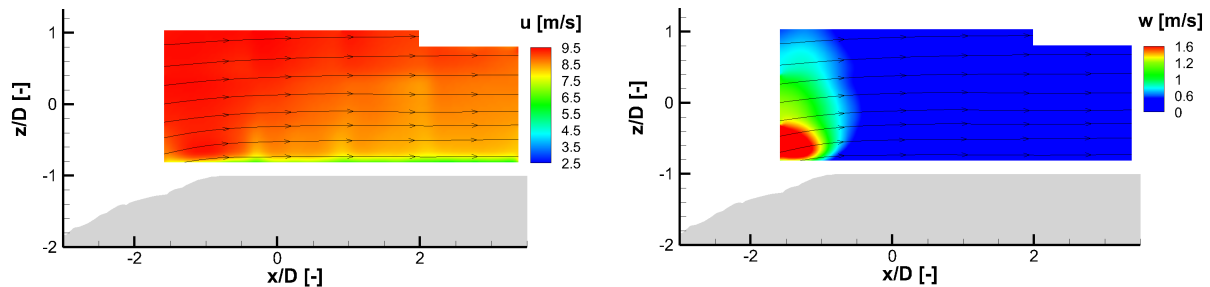


Figure 11: Streamwise (left) and vertical (right) velocity contours without the wind turbine.

Figure 12 shows the contours of the normalized speed-up ratio [27], calculated as the ratio between the free-stream velocity component measured by PIV and the inflow velocity profile measured well upstream of the terrain model (see Fig. 10). Looking at the section in correspondence with the wind turbine rotor disk ( $x/D = 0$ ), a speed-up of about 25% of the free-stream wind speed with respect to the inlet velocity evaluated without the effect of the terrain is observed at the hub position. Considering the entire region of the rotor disk shown by a black line in Fig. 12, the effect of the terrain results in a consistent increase of the free-stream speed between 18% at the top edge and 37% at the lower edge of the disk.

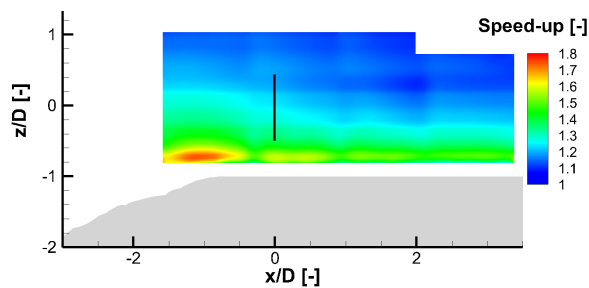


Figure 12: Speed-up ratios at the longitudinal plane; the black line indicates the position of the wind turbine rotor disk.

prior measurements in an atmospheric boundary layer at Technical University of Munich with almost identical inflow characteristics ( $\alpha = 0.18$ , turbulence intensity at hill height 12%) while the complex terrain results have been corrected for blockage effect. Results show a good agreement at  $x/D = 1$  downstream of the rotor for the most part of the wake, except for the lower region where, for the flat terrain case, the velocity is lower. This can be attributed to a reduction in the boundary layer thickness after the escarpment [6], which results in a smaller part of the rotor operating within the boundary layer. At  $x/D = 3$  it can be observed that, apart from the already reported difference close to the terrain, the wake recovers slightly faster for the flat terrain case. This could be explained by a reduction in the turbulence intensity caused by the terrain induced acceleration, even though such a claim requires further investigation.

The flow with the turbine model is illustrated in Fig. 13. The aim here is to analyse the turbine wake behaviour and the impact of the terrain on wake propagation. The velocity deficit behind the turbine along the rotor centerline is clearly seen by looking at the shaded blue contours. The free-stream speed is reduced by ca. 60% at  $x = 1 D$  and 50% at  $x = 3 D$  at the hub height with respect to the case without the wind turbine. Figure 14 shows vertical profiles of the normalized streamwise velocity  $u/U_{hub}$  at  $x/D = 1$  and  $x/D = 3$  downstream of the wind turbine for the complex and flat terrain cases. The flat terrain data are taken from



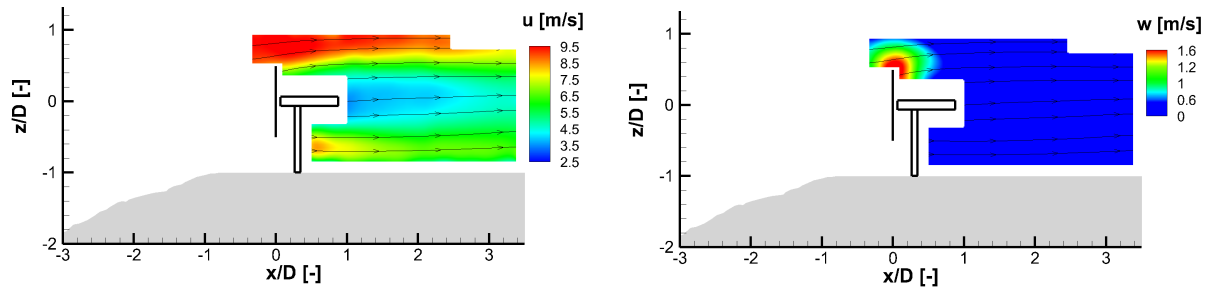


Figure 13: Streamwise (left) and vertical (right) velocity contours with the wind turbine.

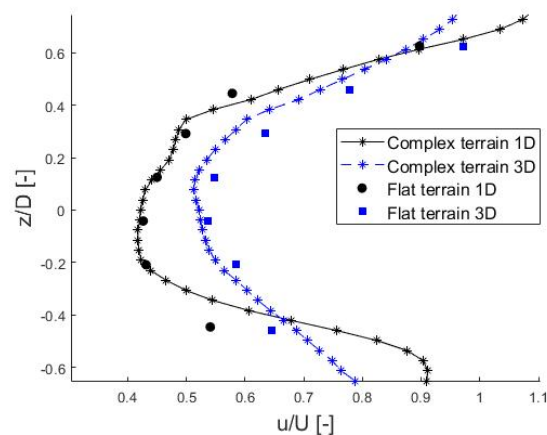


Figure 14: Comparison of vertical wake profiles at 1 D and 3 D between the complex terrain and flat terrain cases.

#### 4. Conclusions

A scaled model of a complex terrain test site was designed and manufactured taking flow similarity criteria into consideration. CFD simulations were used for refining the terrain geometry to ease the manufacturing of the wind tunnel model as well as for evaluating the blockage effect of the terrain when placed in the wind tunnel. The resulting terrain geometry ensures a Reynolds independent flow, while it induces a 5% increase of the wind speed caused by the presence of the wind tunnels walls. The flow over the terrain was measured with PIV with and without a scaled wind turbine model. Initial results without the turbine showed that the terrain induces a consistent increase of the free stream velocity component at the wind turbine rotor disk position with respect to inlet flow measurements. Moreover, a considerable vertical velocity component about 1 D upstream of the turbine was observed from the measurements, due to the steep slope of the terrain. Measurement results with the turbine showed that this particular complex terrain geometry has only a limited influence on the wake, mostly apparent in its lower part close to the ground. In addition, there is a slightly weaker recovery rate about three diameters downstream of the rotor compared to a flat terrain case.

Future steps on this study would be to perform hot-wire and stereo PIV measurements in selected areas of the flow field upstream and downstream of the wind turbine, in order to assess the influence of the terrain on the whole wake area including possible effects on the lateral velocity component. Moreover, a future analysis will include second order statistics, such as turbulence intensity and momentum fluxes that can have considerable effects on wake behaviour (such as

recovery rate) and wind turbine performance. Additionally, the terrain will be equipped with a vegetation model, based on the actual vegetation of the test site, with the aim of experimentally evaluating the effect that this terrain feature can have on the inflow.

## 5. References

- [1] Alfredsson P H and Segalini A 2017 *Philosophical Transactions of the Royal Society A* **375** 20160096
- [2] Lange J, Mann J, Berg J, Parvu D, Kilpatrick R, Costache A, Chowdhury J, Siddiqui K and Hangan H 2017 *Environmental Research Letters* **12** 094020
- [3] Politis E S, Prospathopoulos J, Cabezón D, Hansen K S, Chaviaropoulos P and Barthelmie R J 2012 *Wind Energy* **15** 161–182
- [4] Ayotte K W and Hughes D E 2004 *Boundary-Layer Meteorology* **112** 525–556
- [5] Chock G Y and Cochran L 2005 *Journal of Wind Engineering and Industrial Aerodynamics* **93** 623–638
- [6] Conan B, Chaudhari A, Aubrun S, van Beeck J, Hämäläinen J and Hellsten A 2016 *Boundary-layer meteorology* **158** 183–208
- [7] Jubayer C M and Hangan H 2018 *Journal of Wind Engineering and Industrial Aerodynamics* **175** 65–76
- [8] Li Y, Xu X, Zhang M and Xu Y 2017 *Advances in Structural Engineering* **20** 1223–1231
- [9] Lutz T, Schulz C, Letzgus P and Rettenmeier A 2017 Impact of complex orography on wake development: Simulation results for the planned windfors test site *Journal of Physics: Conference Series* vol 854 (IOP Publishing) p 012029
- [10] Schulz C, Letzgus P, Weihing P, Lutz T and Krämer E 2018 Numerical simulation of the impact of atmospheric turbulence on a wind turbine in complex terrain *Journal of Physics: Conference Series* vol 1037 (IOP Publishing) p 072016
- [11] Schulz C, Lutz T and Krämer E 2018 Aerodynamic response of wind turbines in complex terrain to atmospheric boundary layer flows *New Results in Numerical and Experimental Fluid Mechanics XI* (Springer) pp 753–764
- [12] Hyvärinen A and Segalini A 2017 *Journal of Energy Resources Technology* **139** 051205
- [13] Tian W, Ozbay A, Yuan W, Sarakar P, Hu H and Yuan W 2013 An experimental study on the performances of wind turbines over complex terrain *51st AIAA aerospace sciences meeting including the new horizons forum and aerospace exposition* vol 7 pp 1–14
- [14] Schulz C, Hofsäb M, Anger J, Rautenberg A, Lutz T, Cheng P W and Bange J 2016 Comparison of different measurement techniques and a cfd simulation in complex terrain *Journal of Physics: Conference Series* vol 753 (IOP Publishing) p 082017
- [15] Hofsäb M, Clifton A and Cheng P 2018 *Remote Sensing* **10** 1465
- [16] Wang J, Wang C, Campagnolo F and Bottasso C L 2018 *Wind Energy Science under review*
- [17] Wang C, Wang J, Campagnolo F, Carraón D and Bottasso C L 2018 Validation of large-eddy simulation of scaled waked wind turbines in different yaw misalignment conditions *Journal of Physics: Conference Series* vol 1037 (IOP Publishing) p 062007
- [18] Yeow T S, Cuerva-Tejero A and Perez-Alvarez J 2015 *Wind Energy* **18** 153–169
- [19] Cermac J E 1970 Laboratory simulation of the atmospheric boundary layer Tech. rep.
- [20] Durst F 2008 *An introduction to the theory of fluid flows* (Springer)
- [21] Bowen A 2003 *Journal of Wind Engineering and Industrial Aerodynamics* **91** 1859–1871
- [22] McAuliffe B R and Larose G L 2012 *Journal of Wind Engineering and Industrial Aerodynamics* **104** 603–613
- [23] Snyder W H 1972 *Boundary-Layer Meteorology* **3** 113–134
- [24] VDI 2000 Vdi 3783/12, 2000. environmental meteorology—physical modelling of flow and dispersion processes in the atmospheric boundary layer—applications of wind tunnels
- [25] Nanos E M, Kheirallah N, Campagnolo F and Bottasso C L 2018 Design of a multipurpose scaled wind turbine model *Journal of Physics: Conference Series* vol 1037 (IOP Publishing) p 052016
- [26] Nanos E M, Robke J, Heckmeier F, Jones K, Cerny M, Iungo G V and Bottasso C L 2019 Wake characterization of a multipurpose scaled wind turbine model *AIAA Scitech 2019 Forum* p 2082
- [27] Kilpatrick R, Hangan H, Siddiqui K, Parvu D, Lange J, Mann J and Berg J 2016 *Wind Energy. Sci* **1** 237–254